Sensors & Transducers, Vol. 245, Issue 6, October 2020, pp. 11-19

www.sensorsportal.com

Sensors & Transducers

Published by IFSA Publishing, S. L., 2020
http://www.sensorsportal.com

A LVDT Measurement System for Industrial Applications with Conditioned-Based Maintenance Capabilities

[1, *] Artur M. F. Graxinha and [1, 2] J. M. Dias Pereira

[1] ESTSetúbal, Instituto Politécnico de Setúbal, Setúbal, 2914-761, Portugal
[2] Instituto de Telecomunicações, 1049-001 Lisboa, Portugal
[1] Tel.: +351.265.790000, fax: +351.265.721869
[*] E-mail: artur.graxinha@estsetubal.ips.pt

Received: 31 August 2020 /Accepted: 30 September 2020 /Published: 30 October 2020

Abstract: This paper presents an automatic measurement system for positioning measurements. The system is based on an LVDT transducer and a LabVIEW program was developed for synchronous detection of the LVDT output signal. A complete characterization of the measurement system using a linear actuator was performed in order to obtain accurate metrological values of linearity and hysteresis. The paper will also include data reduction and statistical processing of measurement data to validate the measurement system performance and conformity. An approach for real-time statistical process control of linearity it is presented for measurement system reliability monitoring overtime and, simultaneously, to implement a real-time fault detection and conditioned-based maintenance [1]. It is also important to underline that a preliminary version of the system presented in this paper has been successfully used in electronics automotive manufacturing plants to control the positioning of pointers base on the instrument panel that is a critical operation in cockpits assembly.

Keywords: LVDT, Linearity, Sensitivity, Hysteresis, Synchronous detection, Statistical analysis, Statistical process control, Automotive industrial application.

1. Introduction

Automatic measurement systems [2] have been widely implemented in advanced technological industries. Its metrological capabilities, flexibility, reliability, and low cycle time, enable them to answer simultaneously to the high-quality product specification and high volume production requirements. The emergency of Industry 4.0 [3] highlights the importance of data connection between measurement systems with automatic production cells and information systems. This is, nowadays, a key factor of competitive advantage enabling real process quality control, the statistical analysis and product traceability through serial number barcode reading of RFID [4]. The availability of measurement big data incentives the development of process continuous improvement activities through Lean Six Sigma [5] assisting, at the same time, the engineering program development.

The automotive electronics industry is a typical case where this reality supports a highly competitive environment with tight product specifications and high demanded customer requirements.

This paper describes the development of an automatic measurement system for positioning measurement, based on an LVDT transducer, used during the manufacturing process of electronic instrument panels usually called instrument cluster. In spite of the proliferation of full digital clusters, the use of dc and stepper motors, with pointers assembled, to indicate speed and rpm’s are still the preferred option for high-end series of car makers, due to its metrological attributes.

2. Measurement System

During the electronic cluster manufacturing process, one of the most critical steps is the pointer placement, corresponding to the insertion of the pointer on the motor shaft. This is a meticulous process step that needs to be assisted with a real-time pointer height measurement. The control of the pointer height (distance between the pointer base and graphical scale dial) prevents the occurrence of two distinct failure modes, sticky pointers and loose pointers. Sticky pointer failure mode occurs when the pointer base touches the graphical scale dial, blocking the pointer movement or causing the intermittent pointer displacement. The loose pointers failure mode is the results of a pointer with a high gap between the pointer base and graphical scale dial. In these conditions, the contact area between the pointer hub and the motor shaft is not enough to create retention force to support high torques imposed by motor accelerations.

The novelty of this automatic measurement system [6] relies on the fact that it can be integrated into the typical design of automatic pointer placement machines, with a simple coupling of an LVDT sensor and a data acquisition card connected to the machine computer. All the signal processing and data interchange is done by SW without the requirement of any additional hardware integration. The automatic measurement system enables the accurate real-time measurement of pointer height, during the pointer insertion process, preventing the failure modes occurrence avoiding, that way, further testing when product is fully assembled.

2.1. LVDT

The LVDT transducer, interconnected with blocks of Hardware and Software, is the key element of the measurement system, converting a rectilinear motion of a tool to which is coupled mechanically into a proportional output electrical signal.

Due to de single-axis sensitivity, the LVDT responds to the displacement of the core along the coil's axis. That way, the LVDT can be integrated onto the production system, with the proper mechanical fixtures, sensing the gap between pointer base and graphic scale dial.

The LVDT is an inductive passive sensor with a primary winding centered between a pair of identical secondary windings, with phase inversion, forming the stationary element of the sensor. The moving element is the core of the LVDT made of magnetically permeable material.

The primary winding is supplied with an alternating current defined by,

$$V_i = V_{im} \sin(\omega_0 t), \quad (1)$$

where V_{im} is the amplitude of the signal, $\omega_0 = 2\pi f_0$ and f_0 is the frequency of the input signal. The output signal is the differential ac voltage resulting from the magnetic flux induced by the primary in the two secondary windings, which varies with the axial position of the core within the LVDT coil. The output signal can be described by,

$$V_o = V_{om} \sin(\omega_0 t + \emptyset), \quad (2)$$

where $\emptyset = 180^0$ if V_o is phase shifted in regards to V_i or, $\emptyset = 0^0$ if V_o is in phase with V_i.

As shown in Fig. 1, when the core is located midway between the two secondary windings S1 and S2 the output voltage is zero, since voltage V1 across S1 is equal to voltage V2 across S2.

As core is moved closer to secondary S2 more flux is coupled in S2 resulting that V2 voltage increases while V1 voltages decrease. Within these conditions, V_o is 180^0 phase shifted with V_i. When the core is moved closer to S1 in regards S2, the V1 voltage becomes greater than V2. At this stage V_o is in phase with V_i.

2.2. System Hardware

Fig. 2 represents the hardware elements used in this measurement system. The LVDT Transducer is excited with an external Signal Generator capable of supplying the required LVDT primary input signal. The Oscilloscope enables the visualization of oscillograms of LVDT input and output signals as per Eq. (1) and Eq. (2). The Micrometric Screw works as counter measurement element for the characterization of the LVDT output response function of displacement. The DC Linear Actuator imposes the required linear displacement to the LVDT shaft/core, simulating the precise movement during the pointer placement insertion, supporting, that way, the full characterization of the measurement system. The DC Driver Controller, supplied with a 12 V external power source, supplies the required dc voltage to control the speed and direction (FW-Forward and BW-Backward) of the DC Linear Actuator.

The National Instruments myDAQ acquisition card interfaces with LabVIEW [7] Software through PC/USB. The LVDT input and output signal are also acquired by NI myDAQ for signal processing. The myDAQ controls also the DC Driver Controller with a PWM signal generated with LabVIEW.

2.3. Software

The Software of this automatic measurement system was fully developed using the National Instruments LabVIEW. This SW, made of several LabVIEW subVI's (Virtual Instrument subroutines), aggregates all the elements of the measurement system: The signal acquisition, dc linear actuator and the data measurements collection. The main LabVIEW subVI, represented in Fig. 3, performs the acquisition of the LVDT input and output signals, V_i and V_o, assisted by myDAQ acquisition card.

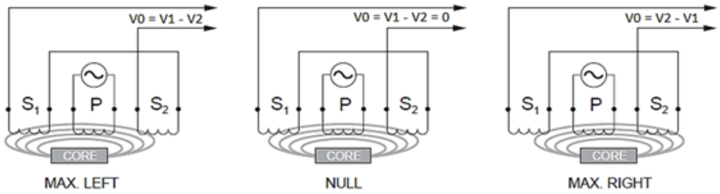

Fig. 1. LVDT core in different axial positions.

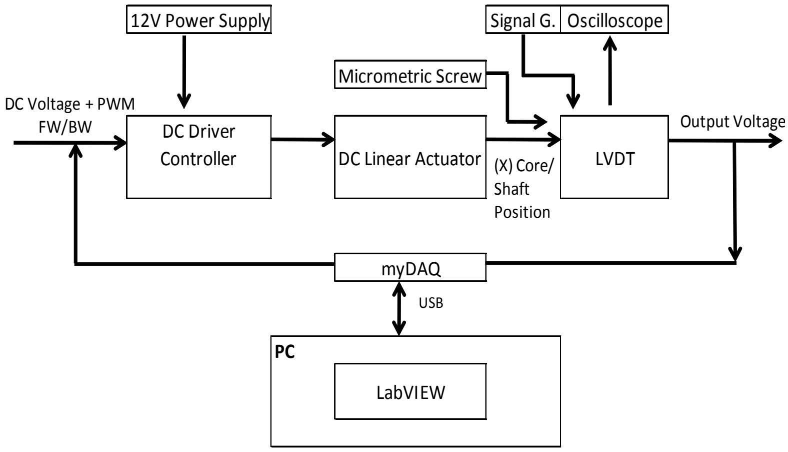

Fig. 2. Measurement System block diagram.

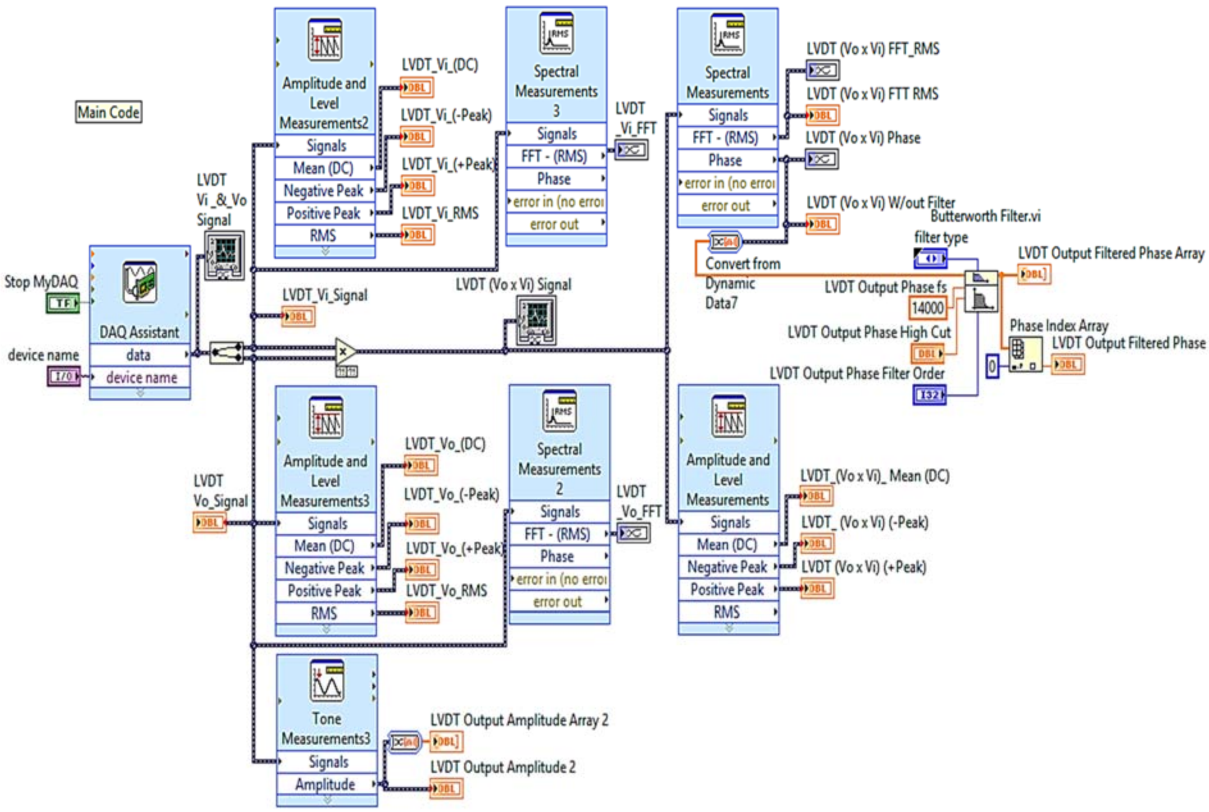

Fig. 3. Main stream software subVI for data acquisition and signal processing.

Once V_i and V_o signals are acquired it is possible to perform an extended range of electric measurements required for the signal processing. For that purpose, it was used the following VI's: DAQ Assistant, Amplitude and Level Measurements, Spectral Measurements and FFT, and a Butterworth 2nd order LPF.

2.4. Synchronous Detection

The synchronous demodulation method was applied to transform the LVDT ac output signal into a dc signal proportional to the displacement of the LVDT shaft/core. To implement this method the LVDT input signal V_i was used as the synchronous signal, for shift lock phase, and its multiplication was performed with the LVDT output signal V_o as described by Eq. (3).

$$V_{im}\,sin(\omega_0 t) * V_{0m}\,sin(\omega_0 t + \emptyset) = \\ = \begin{cases} \frac{V_{im}V_{0m}}{2} - \frac{V_{im}V_{0m}}{2}\cos(2\omega_0 t);\ \emptyset = 0^0 \\ -\frac{V_{im}V_{0m}}{2} + \frac{V_{im}V_{0m}}{2}\cos(2\omega_0 t);\ \emptyset = 180^0 \end{cases}, \quad (3)$$

where $\frac{V_{im}V_{0m}}{2}$ represents the dc component of the output signal. Fig. 4 and Fig. 5 illustrate the oscillograms of the input signal V_i, the output signal V_o and the signal resulting from it's multiplication (V_ixV_o).

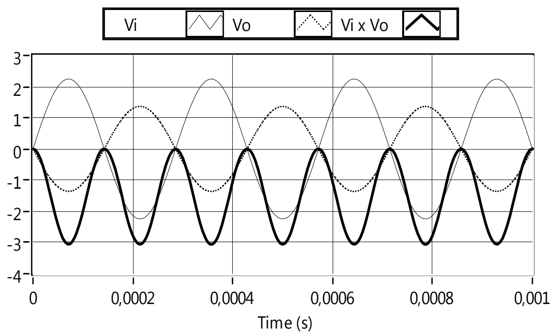

Fig. 4. Input voltageV_i, Output voltage V_o 180º shifted and V_i x V_o.

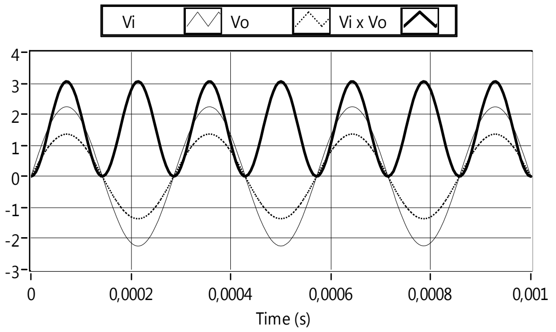

Fig. 5. Input voltage V_i, Output voltage V_o in phase and V_i x V_o.

Using the spectral measurement VI it was possible to obtain the FFT of the input and output signals multiplication and, thus, detect the phase transition of the ac LVDT output between 0º and 180º to obtain a continuous dc output signal, proportional to LVDT shaft/core displacement.

Therefore, re-writing Eq. (3) as,

$$f(t) = \pm\left(\frac{V_{im}V_{om}}{2} - \frac{V_{im}V_{om}\cos(2\omega_0 t)}{2}\right), \quad (4)$$

it can be expanded as a Fourier series [8],

$$f(t) = \\ a_0 + \sum_{n=1}^{+\infty}[a_n\cos(n\omega_0 t) + b_n\sin(n\omega_0 t)], \quad (5)$$

being,

$$\begin{cases} a_n = \frac{2}{T}\int_0^T f(t)\cos(n\omega_0 t)\,dt;\ n = 0\ \ or\ n\ even \\ b_n = \frac{2}{T}\int_0^T f(t)\sin(n\omega_0 t)\,dt;\qquad n\ odd \end{cases}, \quad (6)$$

for n=0 and n=1 we have respectively,

$$\begin{cases} a_0 = \frac{V_{im}V_{om}}{2} \\ a_1 = \frac{V_{im}V_{om}}{2}\,\frac{2}{T}\int_0^T \cos^2(2\omega_0 t)\,dt \end{cases}, \quad (7)$$

where $T = 2\pi/\omega_0$. Fig. 6 represents a_0 and a_1, Eq. (7), obtained with the FFT from signal (V_i x V_o) and define, respectively, the dc component proportional to LVDT core displacement and the amplitude of the first harmonic of the signal. Extracting the rms value of a_1 from Eq. (7) we have:

$$a_{1\ rms} = \frac{V_{im}V_{om}}{2\sqrt{2}} \quad (8)$$

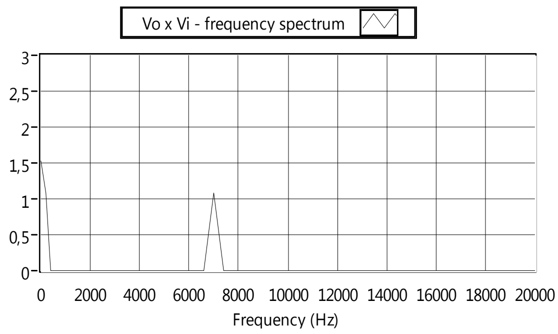

Fig. 6. Frequency spectrum of V_i x V_o.

The Fig. 7 illustrates the synchronous phase-detection demodulating the LVDT output ac signal V_o into a dc continuous signal.

3. Some Results

The dc LVDT output signal (Vdc) enabled the complete characterization of the measurement system that was done in two steps. At a first stage, a Micrometric Screw was used to manually actuate the LVDT shaft/core and, therefore, obtain a complete correlation between physical dimensions in mm and the linear ac LVDT output. At a second stage, the DC Linear Actuator was used, in an automatic sequential way, exercising the LVDT shaft/core to travel back and forward along its full course.

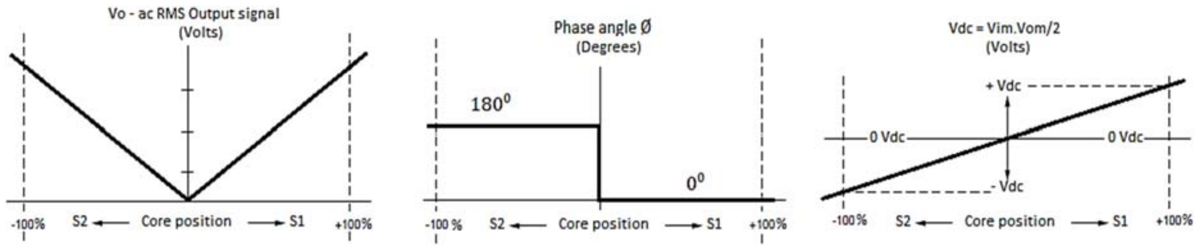

Fig. 7. LVDT output signal conversion from ac to dc.

3.1. Linearity and Sensitivity

Fig. 8 contains the graphic representation of the measurement data taken during the characterization with the Micrometric Screw.

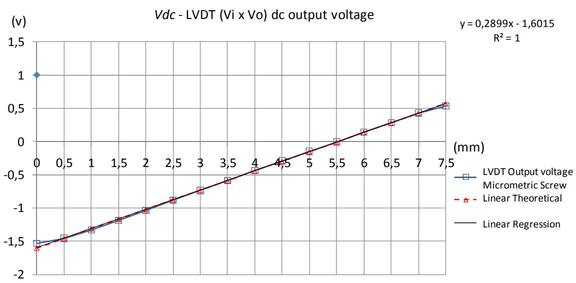

Fig. 8. LVDT characterization, dc output voltage measurements (V) along full shaft/core displacement (mm).

The data was treated statistically and the linear regression equation obtained is defined as:

$$Vdc = 0.2899x - 1.6015, \quad (9)$$

where the variables Vdc and *x* represents, respectively, the LVDT dc output in Volts (V) and the LVDT shaft/core displacement in (mm). The sensitivity obtained is 0.2899 V/mm and the linearity has a maximum local absolute error of 5.6 mV and a maximum local relative error of 1.89 % within the 0.5 mm and 7.0 mm of the LVDT shaft/core course.

3.2. Hysteresis

Table 1 shows the hysteresis absolute and relative errors obtained with the 2 steps of the measurement system characterization described. As it can be seen, the maximum local absolute error is 6.3 mV, representing a relative error of 0.31 %.

Table 1. Data of absolute and relative hysteresis errors.

	Shaft/Core FW motion		Shaft/Core BW motion			
Shaft/Core (mm)	LVDT-Vdc (Vi x Vo) average (V)	Step (V)	LVDT-Vdc (Vi x Vo) average (V)	Step (V)	Hysteresis Abs. Error (V)	Hysteresis Rel. Error (%)
0	-1.5301		-1.5315		0.0014	0.07
0.5	-1.4565	0.0735	-1.4580	0.0735	0.0015	0.07
1	-1.3290	0.1275	-1.3327	0.1253	0.0037	0.18
1.5	-1.1839	0.1452	-1.1845	0.1482	0.0006	0.03
2	-1.0338	0.1501	-1.0374	0.1472	0.0036	0.17
2.5	-0.8845	0.1493	-0.8891	0.1483	0.0046	0.22
3	-0.7359	0.1487	-0.7354	0.1537	0.0004	0.02
3.5	-0.5873	0.1486	-0.5856	0.1498	0.0017	0.08
4	-0.4399	0.1475	-0.4400	0.1456	0.0002	0.01
4.5	-0.2914	0.1485	-0.2909	0.1492	0.0005	0.02
5	-0.1496	0.1418	-0.1463	0.1446	0.0034	0.16
5.5	-0.0068	0.1429	-0.0015	0.1448	0.0053	0.26
6	0.1379	0.1446	0.1410	0.1425	0.0032	0.15
6.5	0.2831	0.1453	0.2894	0.1484	0.0063	0.31
7	0.4280	0.1449	0.4327	0.1433	0.0046	0.23
7.5	0.5323	0.1043	0.5322	0.0995	0.0001	0.01
Max	0.5323		0.5322			
Min	-1.5301		-1.5315			
Span	2.0624		2.0637			

3.3. Statistical Validation of Characterization

In order to validate the LVDT characterization process described in Section 3, it was done the comparison of the linear absolute errors obtained with two actuation methods of the LVDT shaft/core, the manual method with the Micrometric Screw versus the automatic method with the DC Linear Actuator. For this purpose, it was used the sampling data collection obtained with the measurement system. Considering the number of data points used to characterize the linearity (Table 1) and the fact that its statistical distribution is at this stage unknown, it was proposed the use of a statistical non-parametric hypothesis test, the Mann-Whitney-Wilcoxon (MWW) [9].

The MWW tests the differences between the medians of the absolute errors of the two methods. Therefore, being η_1 the median of the linearity error associated with the Micrometric Screw actuation and η_2 the median of the linearity error associated with DC Linear Actuator method, we can define $\eta_1 - \eta_2$ as the median diference between the two methods. Thus, we can define the Null Hypothesis H_0 and the Alternative Hypothesis H_1 as follows:

$$\begin{cases} Ho: \eta_1 - \eta_2 = 0 \\ H1: \eta_1 - \eta_2 \neq 0 \end{cases} \tag{10}$$

Using the statistical SW MINITAB [10] it was possible to apply the MWW bilateral test to the difference of medians with a confidence level of 95 % ($\alpha = 5$ %). As it can be observed on Table 2, it was obtained a P-Value = 0.8. As P-Value > $\alpha = 0.05$ Null Hypothesis H_0 can't be rejected, demonstrating that there are no evidences of statistical significant difference between the medians of the two actuation methods. This result validates the LVDT characterization process used.

Table 2. MWW test summary results.

Test	
Null hypothesis	$Ho: \eta_1 - \eta_2 = 0$
Alternative hypothesis	$H1: \eta_1 - \eta_2 \neq 0$
P-Value	0.8

4. Linearity Control Approach

In the electronic automotive industry the monitoring and control of the metrological characteristics of measurements systems is very demanding, being part of the daily/shifts check lists listed on the Machinery Failure Mode Effect Analysis (MFMEA) [11, 12]. Therefore, at this stage, with the full validation of the automatic measurement system completed, it was important to develop a method to control it linearity stability overtime. As pre-conditions, apart from the required reliability, the method would have to be applied in real-time, without human intervention, avoiding, in that way, the interruption of the production cycle and, consequently, losses on production. In order to achieve that the embedded SW of the measurement system has a routine that, for a configurable time interval, run the measurement system (into a called empty cycle). The objective of this empty cycle is to exercise the LVDT along if full course displacement. The values acquired during this empty cycle will enable to obtain a linear regression equation of the dc LVDT output voltage. The respective values of the "slope" and "Vdc offset" can then be checked using a SPC (Statistical Process Control) [13-15] approach. This is the methodology that is going to be explained now.

Taking benefit from the automatic mode of the measurement system, there were taken more than 900 sequential sample cycles of dc LVDT output signal. From this sample size it were segregated only the values associated with the forward motion from 0 mm up to 7.5 mm. For each forward cycle of the LVDT it were interpolated the respective linear regression equations. We should underline that the option to consider only the forward motion it was supported by the lower hysteresis error and by the fact that on it real application the measurements in the forward motion are preferred. In this way, the conditions to perform the statistical analysis of the linearity stability are sustained.

4.1. Statistical Analysis of Linearity

Based on the multiple linear regression equations of the LVDT output voltage associated with every single forward cycle, it was possible to determine the mean and standard deviations, respectively, for it "slope" (sensitivity) and it Y intercept (on our case "Vdc offset" when displacement $x=0$). As it can be seen on Fig. 9, the statistical analysis of the data done with MINITAB show us a mean value of 0.2896 (V/mm) for the "slope" with a standard deviation of 0.001365 (V/mm).

In what regards "Vdc offset" the statistical analysis demonstrate a mean value of -1.602 (V/mm) with a standard deviation of 0.001704 (V/mm), as it can be observed on Fig. 10.

Concerning, the data normality assessment of the two distributions, "slope" and "Vdc offset", it was done with the statistical test Anderson-Darling, for a confidence level of 95 % ($\alpha = 5$ %) [16]. Therefore, it was defined the Null Hypothesis H_0 and the Alternative Hypothesis H_1 for the "slope" as follows:

$$\begin{cases} H_0: slope \sim N(0.2896, 0.01365) \\ H_1: slope\ do\ NOT \sim N(0.2896, 0.01365) \end{cases}$$

The Anderson-Darling test for the "slope" normality returned a P-Value of 0.452. As P–Value > $\alpha = 5$ %, we had no conditions to reject H_0, accepting, that way, the Null Hypothesis for which the "slope" ~ $N(0.2896, 0.01365)$, as per Fig. 11.

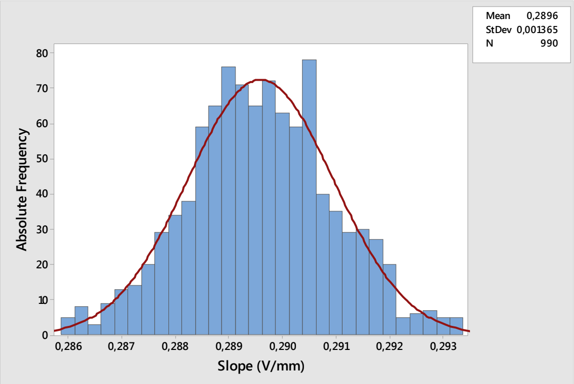

Fig. 9. "Slope" histogram.

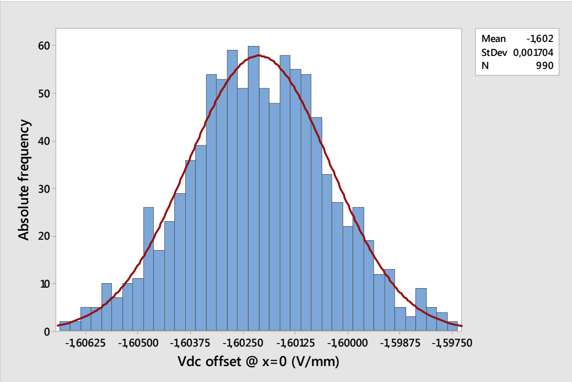

Fig. 10. "Vdc offset" histogram.

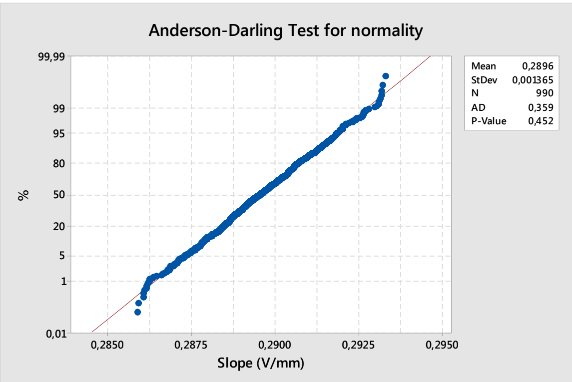

Fig. 11. Anderson-Darling Test for normality for the "slope".

For the "Vdc offset" case we defined the Null Hypothesis H_0 and the Alternative Hypothesis H_1 as follows:

$$\begin{cases} H_0: Vdc\ offset \sim N(-1.60212, 0.001704) \\ H_1: Vdc\ offset\ do\ NOT \sim N(-1.60212, 0.001704) \end{cases}$$

On it turn, the Anderson-Darling test for the "Vdc offset" normality returned a P-Value of 0.885 (Fig. 12).

Once P-Value > $\alpha = 5\ \%$, we have no conditions to reject H0, meaning that we can accept the hypothesis of "Vdc offset" ~ $N(0.2896, 0.01365)$.

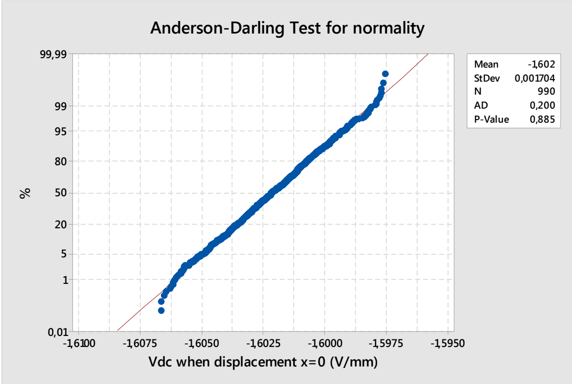

Fig. 12. Anderson-Darling test for normality for "Vdc offset" at displacement x=0 (Vmm).

4.2. Linearity Statistical Process Control

Considering that during the process of data sampling of the sequential sample cycles of dc LVDT output signal for statistical analysis the system have worked only under the effect of the common causes of variation, for which the measured values are only influenced by random noise ~N (0,1).

The time series data of the two characteristics "slope" and "Vdc offset", have not shown evidences of variance changes overtime that could compromise the homoscedasticity, as they didn't show as well presence of data autocorrelation.

Within these conditions was safe to assume that two characteristics followed an IID (Independent and Identical Distributed) process.

4.2.1. Control Charts

Under the conditions described above, we have fulfilled the requirements to control the linearity of the measurement system by monitoring the behavior of the "slop" and "Vdc offset" using individual observation control charts [17-18]. It´s assumed that any effect on the measurement system, in consequence of the presence of special causes of variation, it will immediately impose a variation on the values of the "slope", values of the "Vdc offset" or both, that it will be translated as a point out of the limits of the control charts. The existence of points out of control, in any of these two characteristics, should trigger the equipment shutdown until full elimination of the special cause of variation.

The limits of the individual observations control charts, UCL (Upper Control Limit) and LCL (Lower Control Limit) are defined respectively as follows:

$$\begin{cases} UCL = \bar{X} + 3\sigma \\ LCL = \bar{X} - 3\sigma \end{cases}, \tag{11}$$

where $\bar{X}$ represents the mean value of the variable observation and σ it standard deviation. Thus considering that the "slope" $\sim N(0.2896, 0.01365)$

and the "Vdc offset" $\sim N(-1.60212, 0.001704)$, the control charts limits can be, respectively written as:

$$\begin{cases} UCL = \ 0.293678 \\ LCL = 0.285509 \end{cases} \quad (12)$$

$$\begin{cases} UCL = \ -1.59694 \\ LCL = -1.60731 \end{cases} \quad (13)$$

Fig. 13 and Fig. 14 show, respectively, the multiple sequential observations of the data points referred at Section 4, for the variables "slope" and "Vdc offset". As it can be seen there are no points outside of the control limits demonstrating, therefore, that the measurement system is working uniquely under the presence of common causes of variation with the absence of special causes of variation.

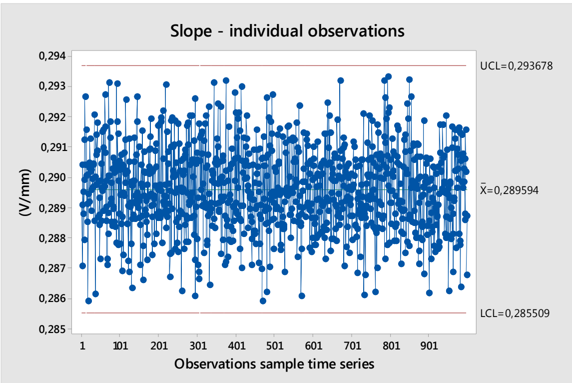

Fig. 13. Control Chart of individual observations for the variable "slope".

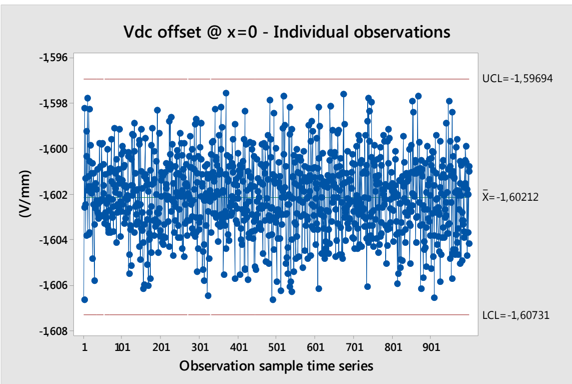

Fig. 14. Control Chart of individual observations for the variable "Vdc offset".

5. Conclusions

The present paper explained how an LVDT can be successfully implemented in the automotive electronics industry. The implementation of this automatic measurement system based on a LVDT with SW Synchronous Detection Capabilities demonstrated, for one side, the good metrological capabilities, with lower errors of linearity and hysteresis and, on the other side, the exceptional flexibility and adaptability to industrial environments technologically advanced, where the interconnectivity of data measurements is fundamental. It was also presented an approach of Statistical Process Control for the linearity of the measurement system. This measurement system enables the real-time process control of the pointer height during the manufacturing of the instrument panels, ensuring at the same time the surveillance of it linearity though real-time SPC, contributing, that way, to the required high quality levels in the electronic automotive industry. Due to the positive results that were obtained, the system has been implemented across the world in multiple automotive electronic plants and is considered one of the best-known methods in its application domain.

Acknowledgements

The author thanks the Systems and Informatics Department of ESTSetúbal/IPS for the availability of the Instrumentation and Measurements laboratory and for the support of the laboratory technician.

References

[1]. C. Chen, B. Zhang, G. Vachtsevanos, Prediction of machine health condition using neuro-fuzzy and Bayesian algorithms, *IEEE Transactions on Instrumentation and Measurement*, Vol. 61, Issue 2, 2012, pp. 297-306.

[2]. Giovanni Spiezia, Roberto Losito, Michele Martino, Alessandro Masi, Antonio Pierno, Automatic Test Bench for Measurement of Magnetic Interference on LVDTs, *IEEE Transactions on Instrumentation and Measurement*, Vol. 60, Issue 5, 2011, pp. 1802-1810.

[3]. T. Stock, G. Seliger, Opportunities of Sustainable Manufacturing in Industry 4.0, *Procedia CIRP*, Vol. 40, 2016, pp. 536-541.

[4]. Patrick Schmitt, Frédéric Thiesse, Elgar Fleisch, Adoption and Diffusion of RFID Technology in the Automotive Industry, *Auto-ID Labs White Paper WP-BIZAPP-041* (http://www.autoidlabs.org).

[5]. Saja Ahmed Albliwi, Jiju Antony, Sarina Abdul Halim Lim, A systematic review of Lean Six Sigma for the manufacturing industry, *Business Process Management Journal*, *Emerald Group Publishing Limited*, Vol. 21, Issue 3, 2015, pp. 665-691.

[6]. Artur M. F. Graxinha, J. M. Dias Pereira, An LVDT Based System with SW Synchronous Detection Capabilities, in *Proceedings of the 6th International Conference on Sensors Engineering and Electronics Instrumentation Advances (SEIA'20)*, Porto, Portugal, 23-25 September 2020, pp. 33-38.

[7]. LabVIEW Web Portal (https://www.ni.com/pt-pt/shop/labview.html).

[8]. C. Ray Wylie, Louis C. Barrett, Advanced Engineering Mathematics, *McGraw-Hill*, Singapore, 1985.

[9]. R. Bergmann, J. Ludbrook, W. P. J. M. Spooren, Different Outcomes of the Wilcoxon-Mann-Whitney Test from Different Statistics Packages, *The American Statiscian*, Vol. 54, Issue 1, 2000, pp. 72-77.

[10]. MINITAB Web Portal (https://www.minitab.com/en-us/products/minitab/).
[11]. William J. Kolarik, Creating Quality, *McGraw-Hill*, New York, 1995.
[12]. AIAG (Automotive Industry Action Group) Web Portal (https://www.aiag.org/quality/automotive-core-tools/fmea).
[13]. D. C. Montgomery, Introduction to Statistical Quality Control, *John Wiley & Sons*, New York, 2013.
[14]. W. A. Levinson, Statistical Process Control for Real-World Applications, *CRC Press*, Boca Raton, FL, USA, 2011.
[15]. M. J. de Smith, Statistical Analysis Handbook, *The Winchelsea Press, Drumlin Security Ltd.*, Edinburgh, Scotland, UK, 2018.
[16]. A. N. Pettitt, Testing the Normality of Several Independent Samples Using the Anderson-Darling Statistic, *Journal of the Royal Statistical Society*: *Series C (Applied Statistics)*, Vol. 26, Issue 2, 1977, pp. 156-161.
[17]. J. Bert Keats, N. Faris Hubele, Statistical Process Control in Automated Manufacturing, Series in Quality and Reliability, *Marcel Dekker Inc.*, New York, 1989.
[18]. D. C. Montgomery, G. C. Runger, Applied Statistics and Probability for Engineers, 5th ed., *John Wiley & Sons, Inc.*, New York, 2011.